AD-A172 229 CORRELATION OF SAW (SURFACE ACOUSTIC WAVE) COATING RESPONSES WITH SOLUBIL (U) NAVAL RESEARCH LAB WASHINGTON DC D S BALLANTINE ET AL. 29 AUG 86 1/1

UNCLASSIFIED NRL-MR-5813 F/G 11/3 NL

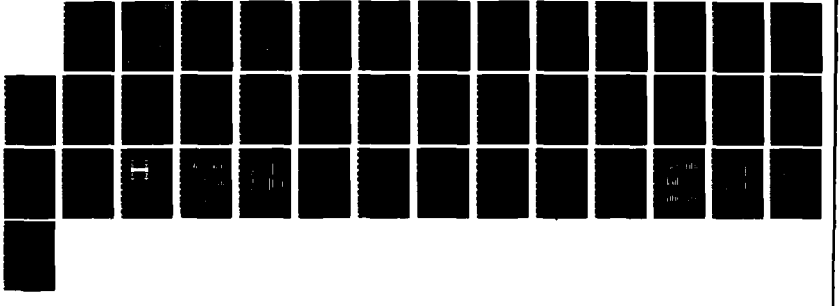

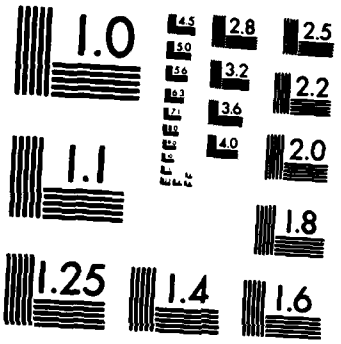

Correlation of Saw Coating Responses with Solubility Properties and Chemical Structure Using Pattern Recognition

DAVID S. BALLANTINE, JR.

Geo-Centers, Inc.
Suitland, MD 20746

SUSAN A. ROSE AND JAY W. GRATE

Surface Chemistry Branch
Chemistry Division

HANK WOHLTJEN

Microsensor Systems, Inc.
Fairfax, VA 22030

86 9 23 088

SECURITY CLASSIFICATION OF THIS PAGE

AD-A172 229

REPORT DOCUMENTATION PAGE

1a. REPORT SECURITY CLASSIFICATION UNCLASSIFIED	1b. RESTRICTIVE MARKINGS
2a. SECURITY CLASSIFICATION AUTHORITY	3. DISTRIBUTION/AVAILABILITY OF REPORT Approved for public release; distribution unlimited.
2b. DECLASSIFICATION/DOWNGRADING SCHEDULE	
4. PERFORMING ORGANIZATION REPORT NUMBER(S) NRL Memorandum Report 5813	5. MONITORING ORGANIZATION REPORT NUMBER(S)
6a. NAME OF PERFORMING ORGANIZATION Naval Research Laboratory 6b. OFFICE SYMBOL (If applicable) Code 6170	7a. NAME OF MONITORING ORGANIZATION
6c. ADDRESS (City, State, and ZIP Code) Washington, DC 20375-5000	7b. ADDRESS (City, State, and ZIP Code)
8a. NAME OF FUNDING/SPONSORING ORGANIZATION Army/CRDC and U.S. Air Force 8b. OFFICE SYMBOL (If applicable)	9. PROCUREMENT INSTRUMENT IDENTIFICATION NUMBER
8c. ADDRESS (City, State, and ZIP Code) Aberdeen Proving Grounds, MD 21010 (Army) Brooks AFB, TX 78235 (Air Force)	10. SOURCE OF FUNDING NUMBERS PROGRAM ELEMENT NO. / PROJECT NO. 61-1439 / TASK NO / WORK UNIT ACCESSION NO.

11. TITLE (Include Security Classification)
Correlation of SAW Coating Responses with Solubility Properties and Chemical Structure Using Pattern Recognition

12. PERSONAL AUTHOR(S)
Ballantine, Jr.,* David S., Rose, Susan A., Grate, Jay W., and Wohltjen,** Hank

13a. TYPE OF REPORT	13b. TIME COVERED	14. DATE OF REPORT (Year, Month, Day)	15. PAGE COUNT
Interim	FROM 6/85 TO 3/86		40

16. SUPPLEMENTARY NOTATION
*Geo-Centers, Inc., Suitland, MD 20746
**Microsensor Systems, Inc., Fairfax, VA 22030

17. COSATI CODES			18. SUBJECT TERMS (Continue on reverse if necessary and identify by block number)
FIELD	GROUP	SUB-GROUP	SAW sensor; Vapor/Coating interactions; Pattern recognition; Coatings testing

19. ABSTRACT (Continue on reverse if necessary and identify by block number)

Twelve surface acoustic wave (SAW) device coatings were exposed to eleven chemical vapors and responses were correlated with solubility properties and coating structure to determine possible vapor/coating interaction mechanisms. Hydrogen bonding ability is implicated as a significant vapor/coating interaction mechanism. Pattern recognition schemes applied to the preliminary data aided in solubility property/response correlations. Principal component analysis demonstrated good separation of different classes of chemical vapors tested. Hierachical clustering provided additional evidence of the correlations between solubility properties and the observed clustering. In addition, pattern recognition methods were used to determine potential selectivity of an array detector using these coatings. Learning techniques show that one fourth of the sensors can adequately separate compounds of interest from chemically similar interferences.

20. DISTRIBUTION/AVAILABILITY OF ABSTRACT ☒ UNCLASSIFIED/UNLIMITED ☐ SAME AS RPT ☐ DTIC USERS	21. ABSTRACT SECURITY CLASSIFICATION UNCLASSIFIED
22a. NAME OF RESPONSIBLE INDIVIDUAL Jay W. Grate, Code 6170	22b. TELEPHONE (Include Area Code) (202) 767-2536 22c. OFFICE SYMBOL Code 6170

DD FORM 1473, 84 MAR 83 APR edition may be used until exhausted
All other editions are obsolete

SECURITY CLASSIFICATION OF THIS PAGE

GPO: U.S. Government Printing Office: 1985-607-047

CONTENTS

CORRELATION OF SAW COATING RESPONSES WITH SOLUBILITY PROPERTIES AND CHEMICAL STRUCTURE USING PATTERN RECOGNITION

INTRODUCTION

Surface acoustic wave (SAW) devices exhibit great potential as small, very sensitive chemical sensors. The principles of operation have been described in detail (1), but they are essentially mass sensitive detectors. They consist of a set of interdigital transducers that have been microfabricated onto the surface of a piezoelectric crystal. When placed in an oscillator circuit, an acoustic Rayleigh wave is generated on the surface of the crystal. The characteristic resonant frequency of the device is dependent on transducer geometry and the Rayleigh wave velocity. Small mass changes or elastic modulus changes on the surface perturb the wave velocity and are readily observed as shifts in this resonant frequency. The extreme sensitivity of these devices makes them attractive as potential gas sensors. The 112 MHz dual SAW devices routinely used in our laboratory, for example, have a theoretical sensitivity of >17 Hz/ng/cm^2. Considering that the active area of the device covers 0.17 cm^2 and assuming a signal to noise ratio of three, this sensitivity results in a minimum detectability of about 0.2 ng (1).

The ultimate performance of a SAW device as a chemical sensor is critically dependent on the sensitivity and selectivity of the adsorbent coating applied to the surface of the piezoelectric crystal. However, no systematic investigation of adsorbent coatings on SAW devices has yet been reported, and references to responses of specific SAW coatings to specific vapors are few in number (2-5). The most closely related sensor technology is

Manuscript approved April 18, 1986.

the bulk piezoelectric crystal sensor, which has been reviewed (6). Coatings exhibiting selectivity to specific vapors have been identified in some cases, but many coatings have been of ill-defined composition and, until recently, selection has been largely empirical (6-11). It is therefore essential to identify coatings for SAW devices which respond to vapors of interest, and to develop a rationale for the selection or design of such coatings.

The development of absorbent coatings alone may not be sufficient for some applications of these devices. It is unlikely that any given material possesses sufficient selectivity to permit accurate detection and identification of a single chemical vapor of interest in the presence of multiple, unknown interferences. A promising approach to this type of analytical problem is the use of pattern recognition techniques in conjunction with an array of sensors of varying selectivity. This approach has been applied to vapor response data from electrochemical sensors (12) and to the selection of coatings for piezoelectric crystal sensors (7).

Pattern recognition techniques, as applied to sensor data, can be described as follows. The sensors encode chemical information about the vapors in numerical form. Each sensor defines an axis in a multidimensional space. Vapors can be represented as points positioned in this space according to sensor responses. Vapors which produce similar responses from the set of coatings will tend to cluster near one another in space. Pattern recognition uses multivariate statistics and numerical analysis to investigate such clustering, and to elucidate relationships in multidimensional data sets without human bias. In addition, the methods can reduce interference effects and improve selectivity in analytical measurements.

In this study, we have generated a large data base consisting of the responses of twelve SAW coatings to eleven vapors at various concentrations, and we have analyzed these data using pattern recognition techniques. Our

objectives were twofold. First, we wished to gather sufficient data to investigate and possibly identify the types of vapor/coating interactions responsible for the observed SAW device responses. Pattern recognition techniques assisted in this effort by clustering vapors with similar response patterns, and by identifying similarities between coatings based on responses to vapors. Secondly, we wished to determine the ability of pattern recognition techniques in conjunction with SAW sensors to discriminate between vapors of interest and chemically similar interferences. Such discrimination is necessary for an array detector to be practical and effective.

EXPERIMENTAL

Materials. Solvents for vapor stream generation were commercial materials of 99.99% purity, except diethyl sulfide (98%-Aldrich) and dimethyl methylphosphonate (97%-Aldrich). These materials are listed in Table I.

The following coating materials were obtained from Aldrich: abietic acid, octadecyl vinyl ether/maleic anhydride copolymer, poly(epichlorohydrin), cis-poly(isoprene), and acrylonitrile/butadiene copolymer (.45/.55). Polyvinylpyrrolidone and OV210 were purchased from Alltech. The two polyphosphazines are proprietary materials and were obtained courtesy of Ethyl Corp. Poly(ethylene maleate) was prepared as described by Snow and Wohltjen [12]. Poly(amidoxime) was prepared by reaction of the acrylonitrile/butadiene copolymer (Aldrich) with hydroxylamine. Subsequent IR analysis indicated a nitrile to amidoxime ratio of .38/.07 (13). Fluoropolyol was prepared using methods described by O'Rear et al. (14). These materials and their structures are given in Table II.

Analytical system. The 112 MHz dual SAW delay lines used in this study were fabricated photolithographically on polished S-T Quartz substrates (1 cm x 1 cm x 0.38 cm thick). The electrodes were made of gold (100 Angstroms

thick) deposited onto titanium (about 200 Angstroms thick) to provide adhesion. Each electrode array consisted of 50 'finger' pairs with each electrode 7 microns wide and spaced 7 microns from the next finger. The electrode arrays had an aperture of 0.224 cm. The devices were clamped into a teflon holder using small pressure clips and screws. A lid attached to this holder was fitted with inlet and outlet tubes to provide a vapor flow path. The two delay lines used in this system were connected as shown in Figure 1.

Dilute solutions of the coating materials were prepared in volatile solvents, usually chloroform, tetrahydrofuran, or a methanol/chloroform mixture. To make chemical sensors, one delay line was coated with the material under investigation using an airbrush. Coating deposition produced frequency shifts of 75-200 KHz, which were recorded and used as a measure of film thickness for normalization and comparison of data (1).

The uncoated delay line acted as a reference oscillator to provide compensation for ambient temperature and pressure fluctuations. Each delay line was connected to a TRW 2820 wideband RF amplifier to provide the amplification required for oscillation to occur. The frequencies obtained from each oscillator were mixed in a double balanced mixer (Mini Circuits Labs SRA-1) to provide the low frequency difference signal which was measured. Frequency measurements were made using a Systron-Donner Frequency Counter Model 6042A. The frequency counter was interfaced to an Apple IIe microcomputer via an IEEE 488 bus and interface card.

Vapor generation system. Vapor streams were generated using an automated gas handler system interfaced with an Apple IIe microcomputer. Plumbing connections were made using 1/8" stainless steel or nickel tubing. The carrier gas was compressed air that was dried by passage through Drierite. Flow rates were controlled with mass flow controllers (Tylan).

Individual vapor streams were generated from one of up to eight bubblers, or one of up to four permeation tubes. Air flow to bubblers was maintained at 39 ml/min, while flow rates to permeation tubes varied from 39-200 ml/min, depending on the desired concentration. Additional air for dilution could be added downstream, up to a total volumetric flow of 1200 sccm. Based on the accuracy of the mass flow controllers, the uncertainties in the total volumetric flow rates were 1.7%. A constant system output of 39 ml/min to the sensor was maintained by a piezoelectric precision gas leak valve. This system will be described in more detail elsewhere (15).

The bubblers consisted of stainless steel vessels containing approximately 100 ml of solvent, with inlet and outlet tubes of 1/8" stainless steel tubing. Vapor mass flow rates were determined by adsorbing the vapor output onto clean, dried charcoal traps. The traps were weighed after 15-20 min collection periods, and mass flows were determined. Two traps in series were periodically used to check for breakthrough. Multiple successive determinations resulted in calculated mass flows (in mg/min) with errors of less than 6%.

A calibrated permeation tube containing methanesulfonyl fluoride was purchased from G.C. Industries (Chatsworth, CA). Permeation tubes containing 1-3 ml of dimethyl methylphosphonate or N,N-dimethylacetamide were prepared using 1 to 1 1/2 inch lengths of Teflon heatshrink tubing (3/8" i.d., Cole-Parmer) capped at both ends with teflon rod. These tubes were stored in a dessicator for 1-3 weeks and then calibrated at operational temperatures (DMMP-50°C, DMAC-25°C). The tubes were weighed every 2-3 days until constant permeation rates (in ug/min) were obtained. Permeation rates had errors of less than 10%.

Data collection and analysis. During coating testing, the difference frequency output of the sensor was recorded every two seconds at 1 Hz

resolution. In a typical experiment, the sensor was exposed to air for one minute to establish a baseline response. This was followed by repeated exposures of vapor/air/vapor/air, with each exposure of two minutes duration.

Each of the twelve coatings was exposed to eleven chemical vapors. Each vapor was run at four different concentrations, with two experiments (four vapor exposures) at each concentration. Frequency shifts caused by these vapor exposures were determined by integrating the area under the signal peak and averaging over the number of data points collected. An equilibration time of 20 min. was scheduled at the beginning of each new vapor to allow the vapor stream to achieve equilibrium. At the completion of the experiments for a given vapor, the gas handler system was flushed with clean air for ten minutes.

Pattern recognition. Since dividing the sensor responses by concentration is not possible for a field instrument measuring unknowns, it was important for each sensor to be exposed to the same concentrations, and to apply a closure method (such as pattern normalization) to the results. The data were collected on individual sensors rather than an array. As a result, the sensor data for a given vapor were not always collected at the same concentration for each sensor. To get the same concentrations for each vapor across a pattern vector, responses for some sensors were interpolated from the calibration curves. For most of the eleven vapors, average frequency shifts were determined for two experiments at each of three concentrations. Only two concentrations resulted in satisfactory responses for MSF, while all four concentrations of DMMP were consistent for all of the sensors tested. These response values, or descriptors, for the eleven vapors formed a 66 x 12 data matrix. Each row in the matrix is a pattern vector, representing responses of the twelve coatings to a given vapor/concentration experiment.

These data were then analyzed on a VAX 11-750 using pattern recognition routines included in ADAPT (16). The pattern vectors were normalized using pattern normalization methods described previously (12). The normalization procedure removes the effects of concentration and the sensitivity of one vapor relative to another. This is necessary to obtain the maximum amount of chemical information from vapors which give only weak responses. Each descriptor for a given coating was then autoscaled to a mean of zero and a standard deviation of unity. Although autoscaling alters the actual values of the sensor responses, it does not alter the number of features or the basic geometry of the clustering (16).

Multiple linear regression was used to investigate the uniqueness of each sensor while testing for collinearities which could cause numerical instabilities in the analysis. After checking the set of sensor responses for collinearities, pattern recognition techniques for display and mapping, clustering, and classification were implemented.

Because it is impossible to imagine the data points clustering in n-dimensional space, a display method was used to transform the data into two-dimensional space for easier visualization. The Karhunen-Loeve transformation finds the axes in the data space that account for the major portion of the variance while maintaining the least amount of error. A correlation matrix for the stored data set is computed and the eigenvalues and eigenvectors are then extracted. The two-principal-component plot presents the plane that best represents the data (17). For display purposes, a non-linear mapping routine is used to separate vapors that overlap when projected onto this plane, but are separated in the multidimensional space. The non-linear mapping routine transforms a set of points from n-space to two-space by maintaining the similarities between the points. It does this by minimizing an error function (18).

Clustering techniques, which are unsupervised learning techniques because the routines are given only the data and not the class membership of the points, group compounds together according to some criterion. By examining the different clustering results, a clearer insight is gained into the actual clustering in n-space (17). ADAPT includes a variety of agglomerative hierarchical clustering routines which group the data by progressively fusing them into subsets, two at a time, until the entire group of patterns is a single set. The routines maintain a particular within-group homogeneity, depending on the criterion and the fusing strategy used. Three dissimilarity metrics were used: a) Euclidean distance squared, b) Euclidean distance, and c) Canberra distance. The fusing strategies investigated were a) nearest neighbor, b) median, c) average, and d) flexible fusion. Resulting data are displayed in dendrograms (19).

Classification methods, which are also considered supervised learning techniques because they are given both the data and the correct classification results, generate mathematical functions to describe the clustering. There are two basic modes of operation for classification methods: a) parametric, and b) nonparametric. Parametric techniques use statistical information based on the underlying data to define the boundaries of the clusters. Their performance is based on the assumptions made concerning the statistical characteristics of the data. The nonparametric techniques use mathematics to define the area between the clusters. The primary parametric programs used in these studies are Bayes linear and quadratic (17), while the nonparametric routines were the perception (17) and adaptive least-squares (ALS) (20).

To achieve the best classification results, each sensor response is multiplied by a constant so that the contribution of each sensor is weighted. The vector that is generated is called a weight vector. The routine iteratively locates the weight vector, and a decision surface can be located

between the classes. The weight vector for a linear decision surface can be generated by one classifier, stored, and then used subsequently in another classifier. Weight vectors can be improved by passing them between classifiers.

Learning techniques are used to train the algorithm on the correct classification results. A discriminant function is found that separates one class from another. The width of the function is a measure of the separation. Feature selection is used to reduce the number of sensors to the smallest set while maintaining good classification results (14). One feature selection method randomly removes vapors from the data set for each analysis in multiple applications of the perception algorithm. As each vapor is removed, the variance in the weight vector is determined. If the observed variance is large, then the information from the corresponding sensor does not contribute significantly to the observed separation of classes.

RESULTS

Vapors used during this study are given in Table I. These vapors were chosen to represent a variety of structural and functional groups. In addition, we were specifically interested in coatings that would be sensitive to toxic organophosphorous compounds. The set of vapors contains three vapors selected as simulants of these materials. Methanesulfonyl fluoride is an irreversible enzyme inhibitor and, as such, exhibits biological activity similar to the organophosphorous insecticides (21). Dimethylacetamide has solubility properties that are similar to these materials, as indicated by the solubility parameter values in Table I. Dimethyl methylphosphonate (DMMP) is structurally similar to many of the organophosphorous pesticides. These three vapors are grouped together and labeled Class 1 vapors. The remaining vapors

are called Class 2 and represent a very general set of potential interferences. Note that tributyl phosphate is also an organophosphorous compound. It has been included in Class 2 specifically to test the ability of the coatings and pattern recognition techniques to distinguish between chemically similar compounds. Included in the table are solvatochromic parameters, which are a scale for comparing the solubility properties of these vapors (22,23). These parameters are a measure of the dipolarity/polarizability (π *), hydrogen bond donor acidity (α), and hydrogen bond acceptor basicity (β). The range of values in the tables are evidence of the generality of the set of selected vapors. No data are available directly for DMMP or isooctane. Values in the table for DMMP are based on values for a similar compound, dimethyl ethylphosphonate (DMEP). Values for isooctane are based on values for 2,4-dimethyl pentane. These parameters will be correlated with observed response behavior in the discussion section.

Adsorbent coatings exhibited good response times, usually reaching 90% of total response within 1 minute. At high vapor concentrations, the response time was more a function of the system dead volume than of the coating response behavior. At lower concentrations, however, responses may have been affected by longer equilibration time between vapor and coating, or by adsorption of vapor onto tubing walls. Upon removal of the vapor stream, a rapid return to a stable baseline was usually observed. A typical response is shown in Figure 2. Reversible responses were observed for all vapor/coating pairs given in Table III. Frequency shift data were used to generate calibration curves. The slopes of these curves, in Hz/ppm (vapor), were then normalized by dividing by the film thickness (in KHz). Normalized responses are presented in Table III.

Coating materials and their structures are given in Table II. Because we were interested in detecting organophosphorous compounds, coatings were

selected based on preliminary tests which indicated a sensitivity to DMMP. Coating sensitivities to other vapors in this study were not known, and extreme selectivities to DMMP and other Class 1 vapors were not suspected. In general, most of the coatings were more sensitive to Class 1 than to Class 2 vapors, and exhibited particularly good sensitivity to DMMP. Poly(ethylene maleate) and fluoropolyol were the most sensitive coatings for detecting DMMP and other Class 1 vapors. The response of fluoropolyol to DMMP was the response of greatest magnitude in the entire data set, and was at least 2000 times greater than its response to any Class 2 vapor. The coating which was least sensitive to DMMP was polyvinylpyrrolidone. While it was the most sensitive coating for water, its response to water was still 10 times less than its response to DMMP.

Noise levels of 10-15 Hz are associated with the SAW devices. Assuming a S/N ratio of 3, the minimum detectable signal is 45 Hz. For a 100 KHz film of fluoropolyol, for example, this translates into detection limits of 0.03 ppm for DMMP and > 2000 ppm for water. For a 100 KHz film of polyvinylpyrrolidone, these detection limits are 11 ppm and 100 ppm, respectively.

Individual bar graphs showing the relative responses of the twelve coatings to six of the vapors are shown in Figure 3. For display, responses are normalized to the coating with the greatest response, while the scale of actual response (in Hz/ppm/ KHz) are given on the y-axis. Similarly, bar graphs showing the responses of four of the coatings to all eleven vapors are shown in Figure 4. The solid bars shown are all normalized to the vapor eliciting the highest response. In most cases, the Class 2 vapors elicited much lower responses than Class 1 vapors. For this reason, the response patterns for these vapors are not easily seen when plotted on the same scale as the Class 1 vapors. To display the relative responses of the Class 2 vapors on the same graph, the Class 2 vapors were normalized to the highest Class 2

response. Cross-hashed bars have been superimposed in Figure 4 to show the response pattern of the normalized Class 2 vapors.

Additional bar graphs illustrating the relative response patterns of individual vapors and coatings are included in the Appendix.

Pattern recognition. The multiple linear regression results indicate that the correlation between sensors are not strong, so individual coatings could not be eliminated on the basis of redundancy. According to eigen-analysis, ten sensors account for 99% of the variance, indicating that at least two of the sensors can be removed without reducing the separation between compounds. The first two-principal-components from the Karhunen-Loeve transformation were used to initialize the non-linear mapping routine. The resulting plot is shown in Figure 5. Class 1 and Class 2 compounds are labeled on the plot with a 1 or a 2, respectively. It is clear that responses for individual vapors tend to cluster in discreet sectors of space with well defined boundaries. In addition, Class 1 vapors tend to cluster near one another. Vapors cluster in n-space based on similarities in response patterns. These clusters may indicate similarities in vapor/ coating interaction mechanisms for these vapors.

Hierarchical cluster analysis produced similar results for each metric. The fusion methods, however, produced different groupings. Flexible fusion was selected for display because it is space conserving and does not change the relationships between the groups of data (24). The dendrogram resulting from hierarchical cluster analysis on one third of the data set is shown in Figure 6. The original matrix was reduced to simplify visualization. Results from the second experiment of the two highest concentrations were selected. The y-axis of the dendrogram is a measure of the dissimilarity of response patterns for given vapors. Thus, diethyl sulfide and toluene exhibit very similar response patterns, and the lines representing the response patterns

for these vapors converge very low on the y-axis of the dendrogram. Conversely, the lines for water and isooctane don't converge, indicating very dissimilar response patterns.

Similarities and dissimilarities in the coatings were examined by applying cluster analysis on the transpose of the 66 x 12 matrix. Since no structural information was available for the polyphosphazine coatings, information derived from these coatings is of limited value. Disregarding the response data for these coatings, cluster analysis was also applied to the transpose of the resulting 66 x 10 matrix. These results are displayed in Figure 7.

Using classification routines and feature selection to reduce the sensors with the most variance, four coatings were found that could separate Class 1 from Class 2 vapors. These were poly(ethylene maleate), fluoropolyol, octadecylvinyl ether/maleic anhydride copolymer, and polyvinylpyrrolidone. The hyperplane between the two classes can be given a dead zone (or a width of 1000 times the normal width produced by the routines), which indicates that the classes are well separated. Using all four coatings, 100% recognition of vapors as Class 1 or Class 2 is possible. Eliminating octadecylvinyl ether/maleic anhydride copolymer decreases this to 94%, which still represents reasonably good discrimination. The weight vectors for these coatings are given in Table IV. Of these coatings, fluoropolyol and polyvinylpyrrolidone are most important for the correct classification of Class 1 vapors, while poly(ethylene maleate) is important for Class 2 vapors.

The non-linear mapping plot from the two-principal-components using these four coatings is shown in Figure 8. While the cluster spaces for some of the vapors appear to overlap, the boundary for Class 1 compounds is still well defined. The dendrogram produced by Euclidean metrics and flexible fusion for these coatings is given in Figure 9. Class 1 compounds are clustered very

closely, and except for butanone, are well separated from the interference vapors.

DISCUSSION

In the course of discussing these results we will attempt to develop a rationale to be used in future coating design and/or selection. The solvatochromic parameters in Table I represent a relative scale for comparing solubility properties of the vapors. By correlating observed responses with these parameters we hope to identify the vapor/coating interaction mechanisms which are responsible for our results. Since no quantitative scale is available to characterize the solubility properties of the coating materials, qualitative estimates of relative hydrogen bond acceptor (HBA) and hydrogen bond donor (HBD) strengths were made based on the weight percentages of HBA and HBD functional groups in their structure. These percentages are reported in Table II. Materials lacking any hydrogen bonding functional groups were labeled non-hydrogen bonding (NHB). All these materials are polymers with the exception of abietic acid, which is a crystalline organic material. Since no structural information was available for the polyphosphazines, results for these coatings will not be included in the discussions of structure/response correlations.

The vapor/coating interaction could be modeled as the dissolution of a solute vapor in a solvent coating. In this model, the response should be determined by solubility interactions, e.g. dipole-dipole and hydrogen bond interactions. The data set as a whole indicates that the solubility properties represented by the parameters in Table I are important in determining SAW device responses. The six vapors whose response patterns are illustrated by the bar graphs in Figure 3 are representative of various classes of vapors, based on solubility properties. Water is a strong HBD and

a weak HBA; n-butanol is both HBD and HBA; DMMP and tributyl phosphate are HBA but not HBD; isooctane is a NHB vapor with little or no dipolarity/polarizability; and dichloroethane is a NHB vapor with significant dipolarity/polarizability. The bar graphs in Figure 3 show that vapors with different solubility properties elicited different coating response patterns. Vapors with similar solubility properties, such as DMMP, dimethylacetamide and 2-butanone have more similar response patterns (see data in Table III). DMMP and tributyl phosphate, however, have easily distinguishable response patterns but have similar solubility properties. Closer examination shows that this is primarily due to polyvinylpyrrolidone, fluoropolyol, and OV210, while the remaining coatings give a more similar pattern for these vapors.

The reason for which all the coatings were most sensitive to DMMP is not clear. Examination of the solubility parameters in Table I indicates that DMMP is exceptional in neither its hydrogen bonding ability nor its dipolarity/polarizability. Therefore, the extremely high response of these coatings to DMMP must be due to some solubility property which has not been characterized in Table I, or to a fortuitous combination of solubility properties.

Hierarchical cluster analysis provides a more systematic determination of the similarity or dissimilarity of the various vapors, as determined by SAW sensor responses. The resulting dendrogram in Figure 4 sorts the vapors in a manner which is consistent with their solubility properties. Starting from the top of the plot and working down (toward increasing similarity), the NHB vapors on the right are separated from the HBA and HBD vapors on the left. Isooctane is separated from the other NHB vapors, a result consistent with the unique character of isooctane as indicated in Table I. It is the only vapor with near zero dipolarity/polarizability. The NHB vapors with significant dipolarity/polarizability (1,2-dichloroethane, toluene, and diethyl sulfide)

are more similar to one another than they are to isooctane or the HBA and HBD vapors. In this cluster, dichloroethane stands out in the dendrogram and in Table I as the NHB vapor with the greatest dipolarity/polarizability.

Among the HBA and HBD vapors on the left of the dendrogram, water is the least similar to any other vapors. Accordingly, water is seen in Table I to have extremely high dipolarity/polarizability. It is also unusual in its relatively high HBD character. The other HBD vapor, n-butanol, has significantly greater HBA character and less dipolarity/polarizability than water, and is shown in the dendrogram to be more similar to the other HBA vapors. In general, the HBA vapors cluster together, with DMMP and dimethylacetamide being the most similar. These results demonstrate that the solubility properties in Table I should be considered as important factors affecting SAW sensor responses.

Exceptions to these general trends must also be considered. For example, methanesulfonyl fluoride clusters with the other HBA vapors, but it is a weak HBA vapor and may be more similar to that of diethyl sulfide, a NHB vapor. Similarly, tributylphosphate does not cluster as closely to DMMP as might be expected based on the fact that both are organophosphorous compounds with similar HBA strength. Individual comparisons, therefore, emphasize the importance of factors in addition to the solubility properties in Table I.

The roles of coating properties and structures in determining sensor responses cannot be fully determined by these data. Coating responses will be influenced by a mixture of interactions with various structural features such as double bonds, conjugation, aliphatic side chains, and heteroatomic functional groups. The relative importance of these interactions is difficult to determine, and relevant solubility properties for these coatings have not yet been identified.

We can, however, explore the role of hydrogen bonding interations by using the relative scale of HBA and HBD strengths in Table II. With the exception of poly(isoprene), all of the coatings contain heteroatoms capable of accepting hydroben bonds. HBA strength should be significant for those coatings containing carbonyls or nitrogen-containing groups. Weaker HBA strength is expected for those coatings containing only ether linkages. Three of the coatings also contain HBD groups (fluoropolyol, poly(amidoxime), and abietic acid). Water and butanol are the only HBD vapors in our data set. Of these, trends in the response to water vapor are most likely due to HBA strength of the coatings because water has stronger HBD than HBA strength, and has no aliphatic character. For this reason, coatings were listed on the x-axis of Figure 3 in order of decreasing response to water.

The results in Figure 3 show that the relative coating responses to water tend to follow the relative HBA strengths estimated from the weight percentages of the HBA functional groups in the coating structures. This confirms that hydrogen bonding interactions are important and justifies consideration of the simple scale in Table II. While water also has considerable dipolarity/polarizability properties, the data indicate no correlation with polarity. Nonpolar isooctane does not exhibit a trend opposite to that exhibited by water, nor does polarizable dichloroethane follow any apparent trend. The other HBD vapor, n-butanol, exhibits a different response pattern. This may be due to greater HBA strength and more organic character relative to water.

On the low end of this scale, poly(isoprene) is the only NHB coating in this study. It exhibits a much larger response to the NHB vapor isooctane than any other coating, with the exception of abietic acid. In addition, the responses of poly(isoprene) to other NHB vapors (dichloroethane, toluene, and

diethyl sulfide) are larger than for the HBA and HBD vapors in Class 2. In general, the other coatings exhibit higher responses to Class 2 HBA vapors, particularly TBP and butanol, than to the NHB vapors.

The bar graphs in Figure 4 and the data in Table III indicate that all the coatings, except polyvinylpyrrolidone, have a fundamental similarity. They are more sensitive to Class 1 than to Class 2 vapors. Cluster analysis helps to more clearly identify similarities and dissimilarities among the coatings. In the dendrogram in Figure 7, fluoropolyol, poly(ethylene maleate), and PVP stand out as being most dissimilar to other coatings, and also dissimilar to one another. These results can be related to the data by examining the bar graphs in Figure 3. Relative to the other coatings, fluoropolyol has very strong response to DMMP, a weak response to water, and average responses to tributyl phosphate and isooctane. Poly(ethylene maleate) exhibits strong response to DMMP, water and tributyl phosphate, and an average response to isooctane. Polyvinylpyrrolidone has strong responses to water and tributyl phosphate, but gives the weakest responses to DMMP and isooctane. In relating the dendrogram results to structure, it is worth noting that polyvinylpyrrolidone may be the most basic of the coatings in the data set. Poly(ethylene maleate) may be the most polar, since it has polar groups in the backbone and no side chains. Fluoropolyol is distinctive in its combination of structural features, such as fluoroaliphatic, aromatic, ether, and hydroxyl groups.

Similarities among the coatings are shown in the dendrogram by the clustering of poly(isoprene), octadecylvinyl ether/maleic anhydride copolymer, and OV210. These all have substantial hydrophobic character. The cluster containing poly(epichlorohydrin), abietic acid, acrylonitrile/butadiene copolymer, and poly(amidoxime) is of interest because poly(amidoxime) is a

modification of the acrylonitrile/butadiene copolymer. The modification created a small percentage (.07) of HBD groups. As a result, poly(amidoxime) clusters slightly closer to abietic acid, which also has HBD groups, than to its parent polymer. A previous study of 27 coating materials on piezoelectric sensors demonstrated that clustering of these materials may be influenced by structural similarities (7). Fewer coatings were used in our data set, and the coatings employed were structurally more diverse. As a result, such clustering is not as evident.

CONCLUSIONS

Solubility properties were systematically demonstrated to be an important factor in determining SAW sensor responses, and currently provide the best rationale for selecting or designing coatings for specific applications. A more detailed investigation of the relationship between structure and observed solubility properties would also facilitate the selection and design processes.

Pattern recognition techniques were valuable in extracting information regarding vapor/coating interactions from this multidimensional data set. In addition, it is clear that the combination of multiple sensor arrays of coated SAW devices and appropriate pattern recognition software will provide a sensor system which can be selective as well as sensitive for a broad spectrum of compounds.

ACKNOWLEDGEMENTS

The authors wish to thank the following persons for their efforts: Peter Jurs, for his guidance in the pattern recognition work; Arthur Snow and James Griffith of the NRL Polymeric Materials Branch, NRL, for supplying us with much of the coating materials and related structures; and M. J. Kamlet and

Michael Abraham for much informative discussion. The coatings testing work was supported by Army/CRDC, Aberdeen Proving Ground, MD. The pattern recognition work was supported by LT Brad Rikke, HG AMD/RDSX, Brooks AFB, TX. Research was performed at Naval Research Laboratory, Washington, D.C.

REFERENCES

1. Wohltjen, H., *Sensors and Actuators* 1984, *5*, 307.

2. Snow, A. and Wohltjen, H., *Anal. Chem.* 1984, *56(8)*, 1411.

3. Bryant, A.; Poirier, M.; Riley, G.; Lee, D.L.; and Vetelino, J.F., *Sensors and Actuators* 1983, *4(1)*, 105.

4. D'Amico, A.; Palma, A.; and Verona, E., *Sensors and Actuators* 1982/1983, *3(1)*, 31.

5. Chuang, C.T.; White, R.M.; and Bernstein, J.J., *IEEE Electron. Device Lett.* 1982, EDL-*3(6)*, 145.

6. Alder, J.F. and McCallum, J.J., *The Analyst* 1983, *108*, 1169.

7. Carey, W.P.; Beebe, K.R.; Kowalski, B.R.; Illman, D.L.; and Hirschfeld, T., *Anal. Chem.* 1986, *58*, 149.

8. Fog, H.M. and Reitz, B., *Anal. Chem.* 1985, *57*, 2634.

9. Morrison, R.C. and Guilbault, G.G., *Anal. Chem.* 1985, *57*, 2342.

10. Guilbault, G.G.; Kristoff, J.; and Owens, D., *Anal. Chem.* 1985, *57(8)*, 1754.

11. Kindlund, A.; Sundgren, H.; and Lundstrom, I., *Sensors and Actuators* 1984, *6*, 1.

12. Stetter, J.; Jurs, P.C.; and Rose, S.L., Accepted for publication in *Anal. Chem.*

13. Jarvis, N.L.; Lint, J.; Snow, A.W.; and Wohltjen, H., "Proceedings of the 1983 Scientific Conference on Chemical Defense Research," CRDC-SP-84014, Eds. Dimmick, R.L. and Rausa, M., U.S. Army, 1984, pp. 45-53, NTIS, ADB-090896L.

14. O'Rear, J.G.; Griffith, J.R.; and Reines, S.A., *J. Paint. Technol.* 1971, *43(552)*, 113.

15. Grate, J.W.; Ballantine, D.S., Jr.; and Wohltjen, H., in preparation.

16. Stuper, A.J.; Brugger, W.E.; and Jurs, P.C., "Computer Assisted Studies of Chemical Structure and Biological Function," Wiley, New York, NY, 1979.

17. Tou, J.T. and Gonzalez, R.C., "Pattern Recognition Principles," Addison-Wesley, Redding, MA, 1974.

18. Beech, G., "Fortran IV in Chemistry," John Wiley, New York, NY, 1975.

19. Massart, D.L. and Kaufman, L., "The Interpretation of Analytical Chemical Data by Use of Cluster Analysis," John Wiley, New York, NY, 1983.

20. Moriguchi, I.; Komatsu, K.; and Matsushita, Y., *J. Med. Chem.* 1980, *23*, 20.

21. Daffron, A.; Neenan, J.P.; Ash, C.E.; Betts, L.; Finke, J.M.; Garman, J.A.; Rao, M.; Walsh, K.; and Williams, R.R., *Biochem. Biophys. Res. Comm.* 1982, *104*, 597.

22. Kamlet, M.J. and Taft, R.W., *Acta Chem. Scand.* 1985, *B39*, 611.

23. Kamlet, M.J.; Abboud, J-L.M.; Abraham, M.H.; and Taft, R.W., *J. Org. Chem.* 1983, *48*, 2877.

24. Williams, W.T. and Lance, G.N., in "Statistical Methods for Digital Computers," Eds. Enslein, K.; Ralston, A.; and Wilif, R., Wiley-Interscience, New York, NY, 1975.

25. Abraham, M.H., personal communication.

Table 1 — Test Vapors and Solubility Parameters

Permeation Tubes - Class 1	π^*	β	α
methanesulfonyl fluoride (MSF)	---	---	---
N,N-dimethylacetamide (DMAC)	.88	.76	0.0
(dimethyl) methylphosphonate (DMMP)[a]	---	(.81)	(0)
Bubblers - Class 2			
1,2-dichloroethane (DCE)	.81	.00	0.0
water	1.09	.18	1.17
isooctane (ISO)[a]	(0.0)	(0.0)	(0.0)
toluene (TOL)	.54	.11	0.0
diethyl sulfide (DES)[a]	.36	.28	0.0
tributyl phosphate (TBP)[a]	.65	.77	0.0
2-butanone (BTN)	.67	.48	0.0
n-butanol (BTL)	.47	.88	.79

[a] These values are unpublished data from Abraham (25). Values in table for DMMP are taken from similar compound, DMEP; values for isooctane are taken from 2,4-dimethyl pentane.

Table 2 — Coating Materials and Structures

COATING	STRUCTURES	HYDROGEN BOND ACCEPTOR-DONOR (% OF TOTAL)
POLY (ETHYLENE *MALEATE) (PEM)*	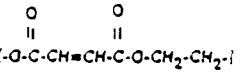	CARBONYL (HBA)-20% *O-LINKAGE (wHBA)*-11%
OCTADECYL VINYL ETHER MALEIC ANHYDRIDE COPOLYMER (OVERMAC)	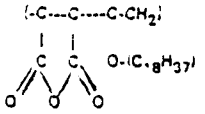	CARBONYL (HBA)-14% O-LINKAGE (wHBA)-8%
	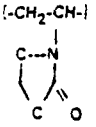	CARBONYL (HBA)-25% N (HBA)-13%
ACRYLONITRILE BUTADIENE COPOLYMER (PBAN)	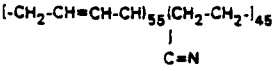	NITRILE (HBA)-22%
POLY (AMIDOXIME) (PAOX)	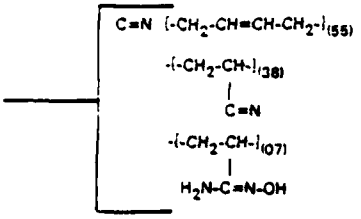	NITRILE (HBA)-19% AMIDOXIME (HBA-D)-3%
POLY(EPICHOROHYDRIN) (PECH)	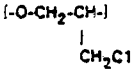	O-LINKAGE (wHBA)-17%
ABIETIC ACID (ABACD)	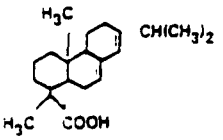	CARBOXYL (HBA-D)-15%
OV210	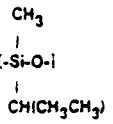	O-LINKAGE (wHBA)-10%
FLUOROPOLYOL (FPOL)	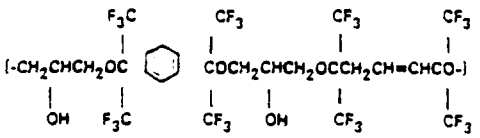	HYDROXYL (HBA-D)-4%
POLY (ISOPRENE) (PIP)	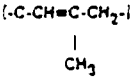	NONE (NHB)
POLYPHOSPHAZINES *PPZN1 PPZN2)*	----	----

Table 3 — Normalized Vapor Responses (10^{-3} Hz/ppm/KHz

VAPORS	COATINGS											
	PEM	OVEMAC	PVP	PBAN	PAOX	PECH	ABACD	FPOL	PIP	OV210	PPZN1	PPZN2
MSF	240	78	44	160	130	0.0	96	390	21	0.0	30	37
DMAC	650	60	0.0	38	290	210	39	1360	15.6	6.4	19	130
DMMP	6500	460	40	450	830	550	590	15800	230	204	340	990
DCE	4.2	0.9	2.0	3.4	4.2	3.0	3.3	2.4	2.5	0.4	0.5	0.9
WATER	2.8	1.3	4.8	0.3	0.4	0.6	0.4	0.2	0.09	0.2	0.2	0.7
ISO	0.7	0.6	0.13	0.4	0.4	0.4	1.9	0.4	1.7	0.3	0.0	0.4
TOL	3.8	1.3	0.7	3.9	4.8	3.9	9.4	0.12	3.7	0.6	0.5	1.4
DES	4.4	1.3	0.4	3.4	4.0	4.1	8.7	3.0	3.7	0.6	0.4	1.7
TBP	24	3.6	33	6.4	17	7.2	13.8	13	0.08	29	3.7	--
BTN	3.6	0.5	0.5	1.8	1.9	2.0	2.2	3.0	0.54	0.3	1.3	1.9
BTL	11	2.7	11	3.4	8.9	2.6	18	8.0	1.0	0.7	0.9	1.1

Table 4 — Weight Vector Components for 4 Best Coatings

Coating	Weight Vector Value	# wrong Class 1	# wrong Class 2	Recognition
----		0	0	100%
OVEMAC	-0.06783	3	1	93.9%
PEM	0.11633	2	8	84.9%
PVP	-0.80966	18	0	72.7%
FPOL	0.20978	14	6	69.7%

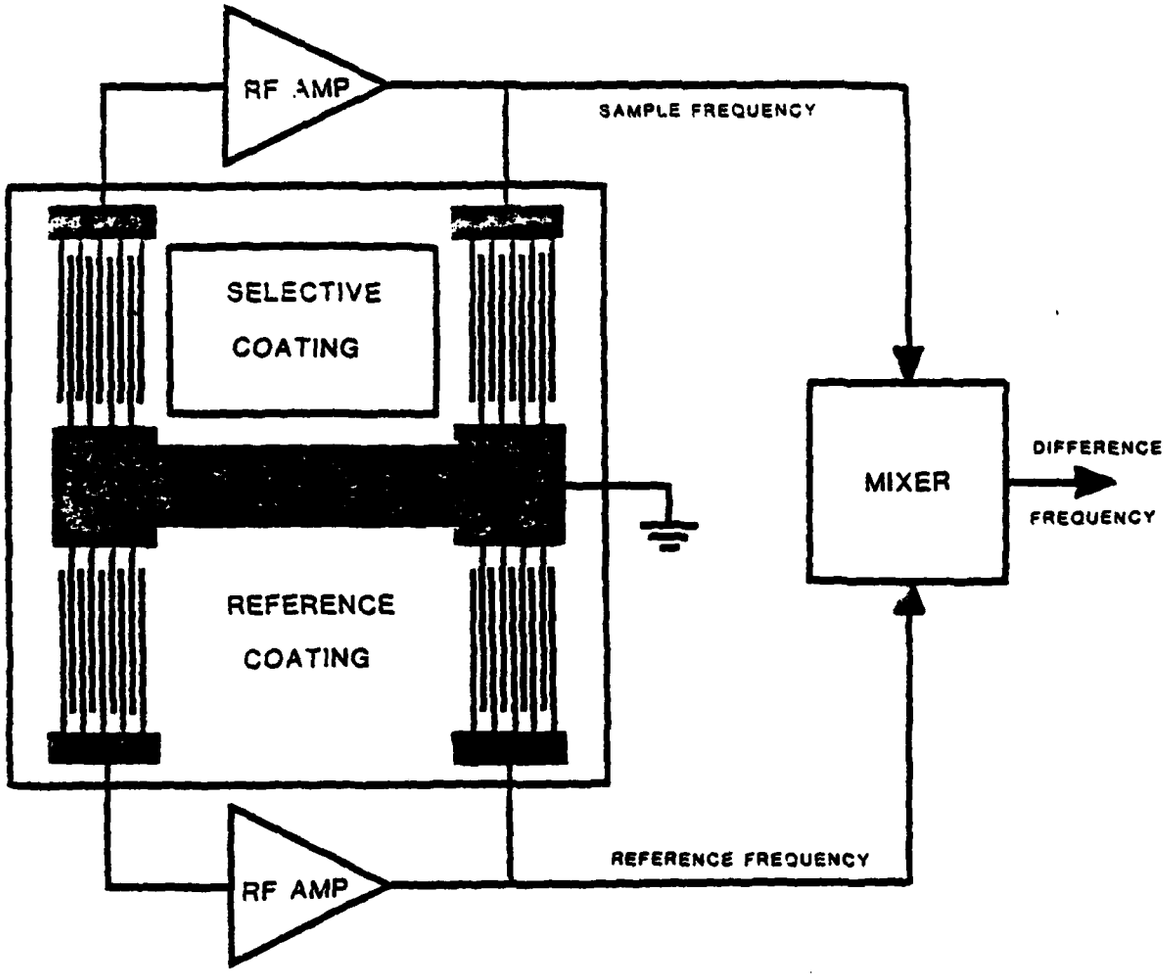

Fig. 1 — 112 MHz SAW device and associated electronic circuit diagram

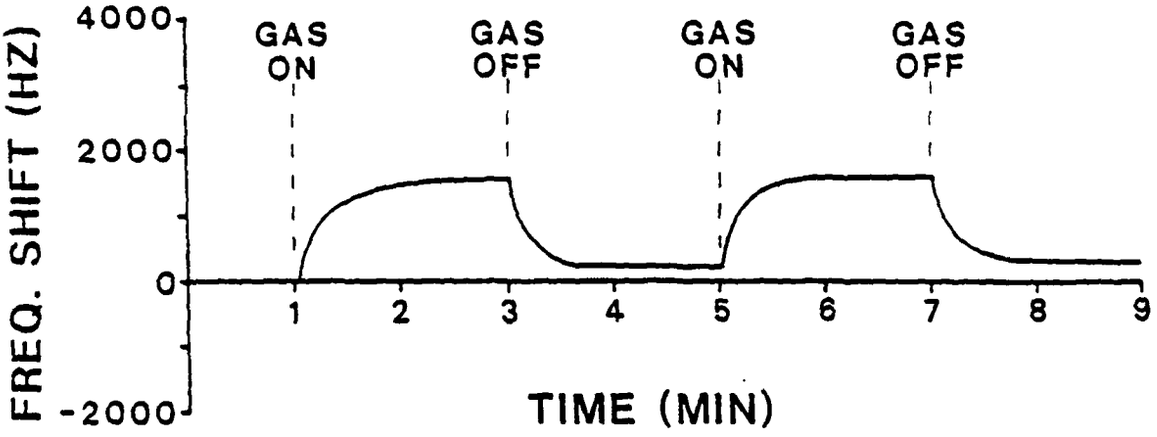

Fig. 2 — Typical SAW device reversible response

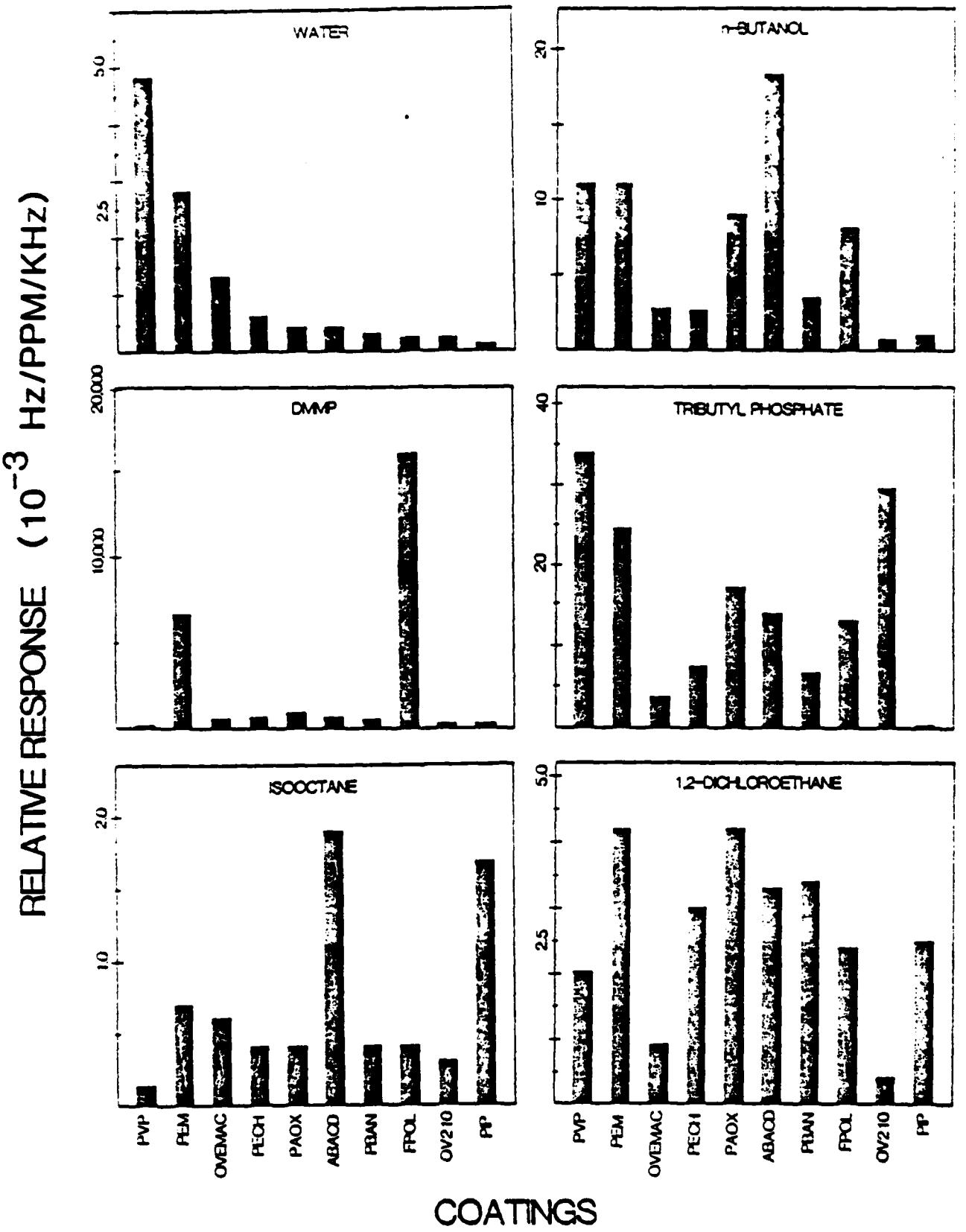

Fig. 3 — Bar graphs showing relative response patterns of 10 coatings to specific vapors

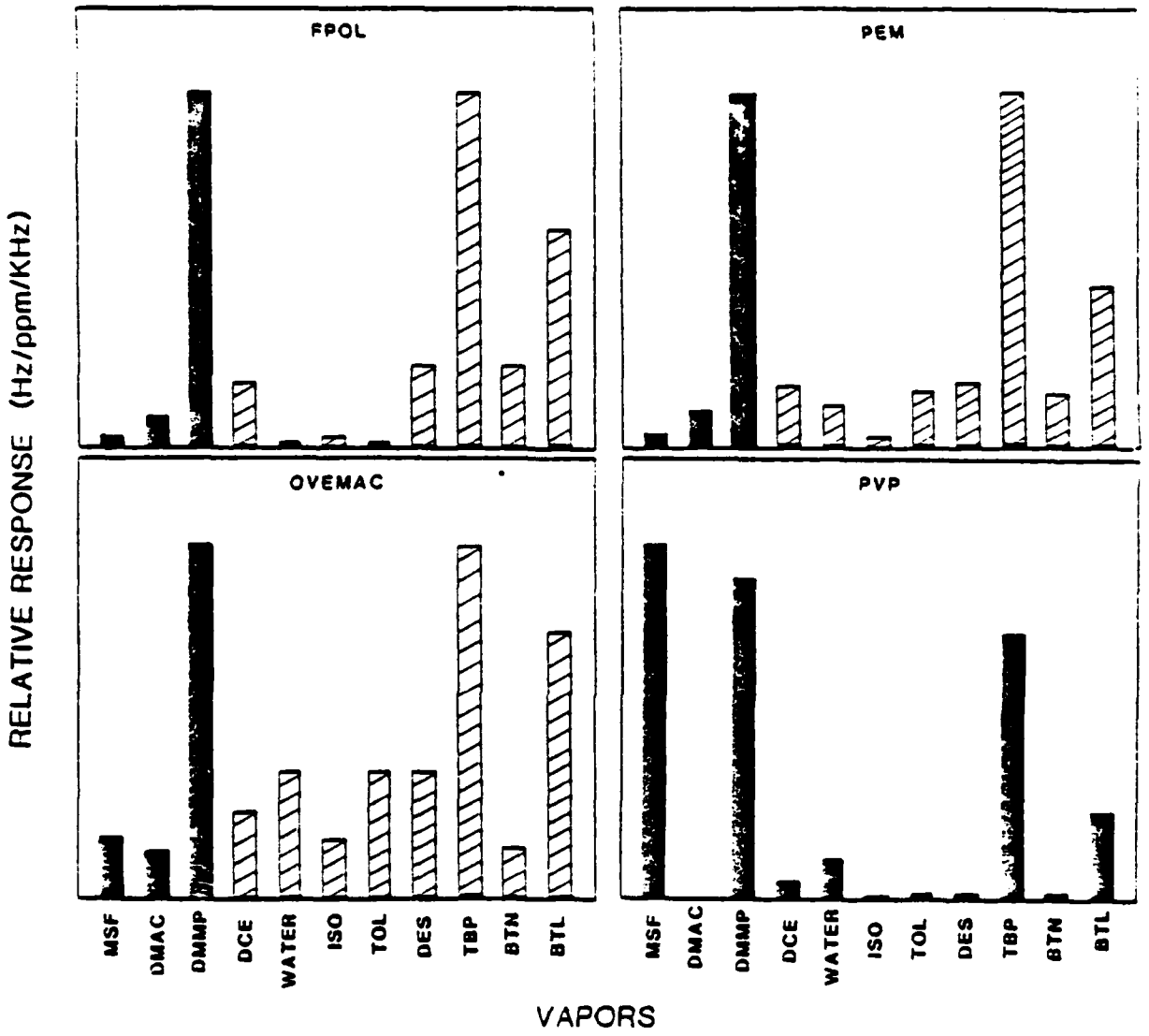

Fig. 4 — Bar graphs showing relative response patterns of 4 coatings normalized to Class 1 vapors (solid bars) and Class 2 vapors (cross-hashed bars)

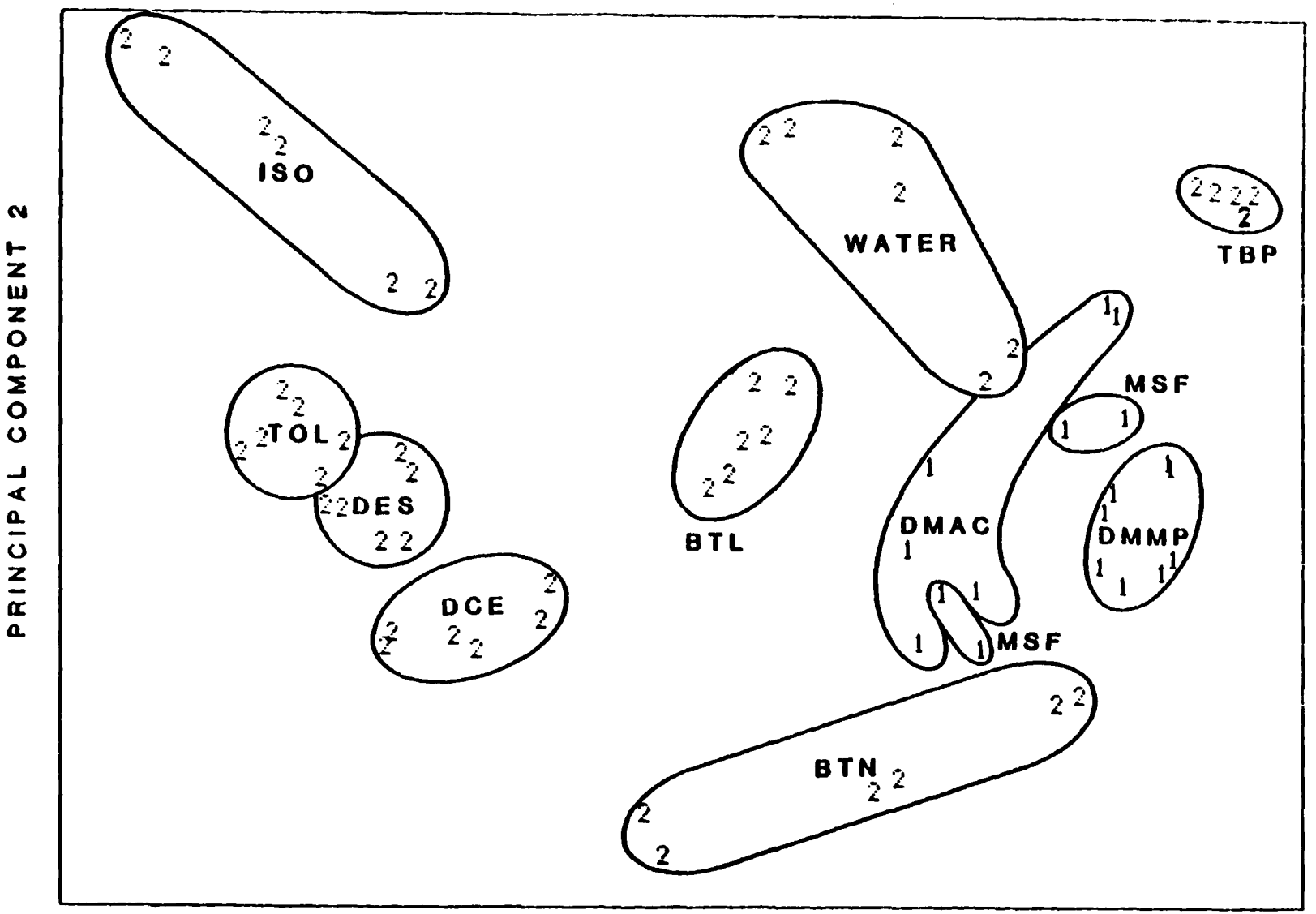

Fig. 5 — Principal component plot using results from all 12 coatings

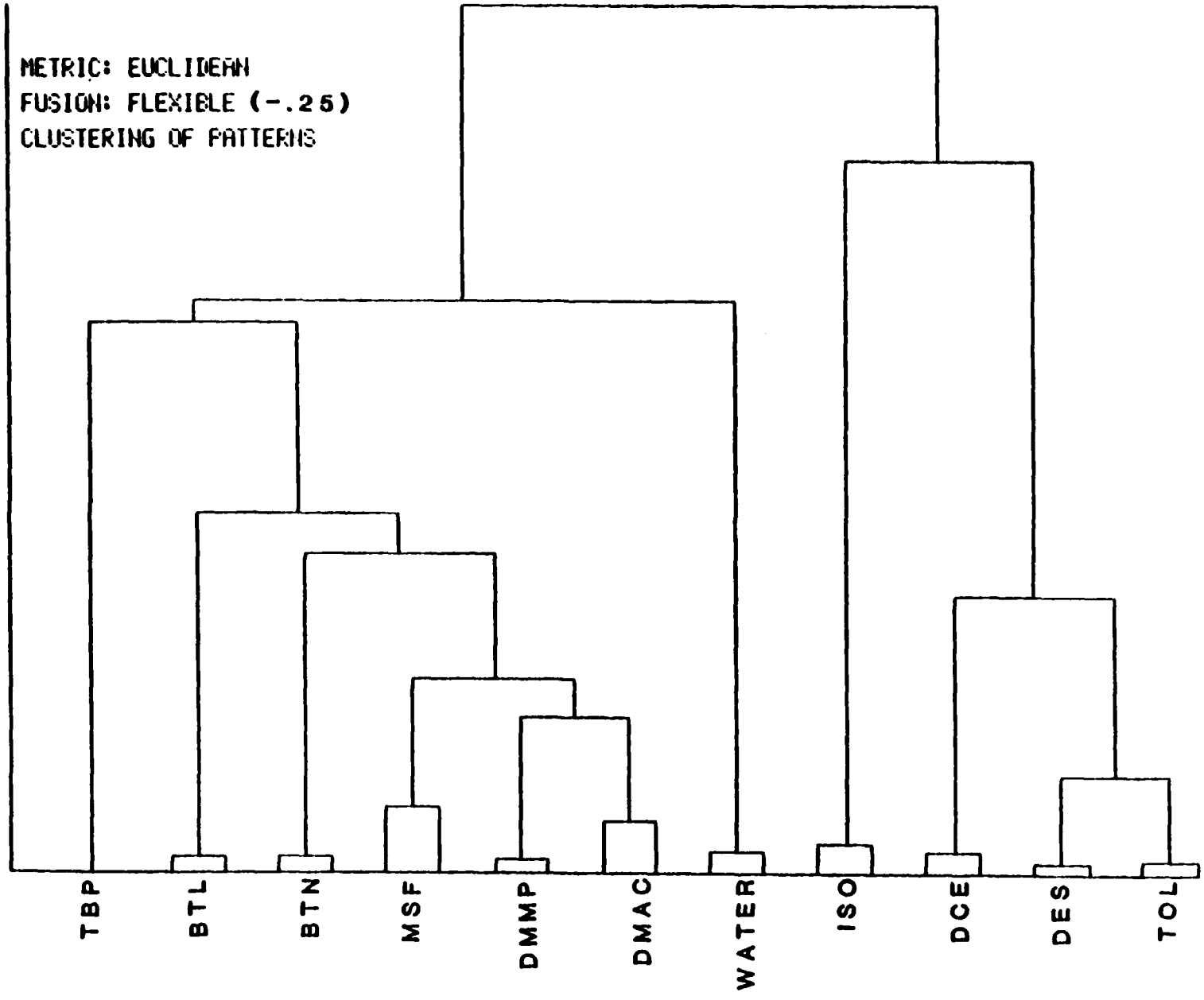

Fig. 6 — Typical hierarchical cluster results of all the vapors based on all 12 coatings (Euclidean distance metric with flexible fusion)

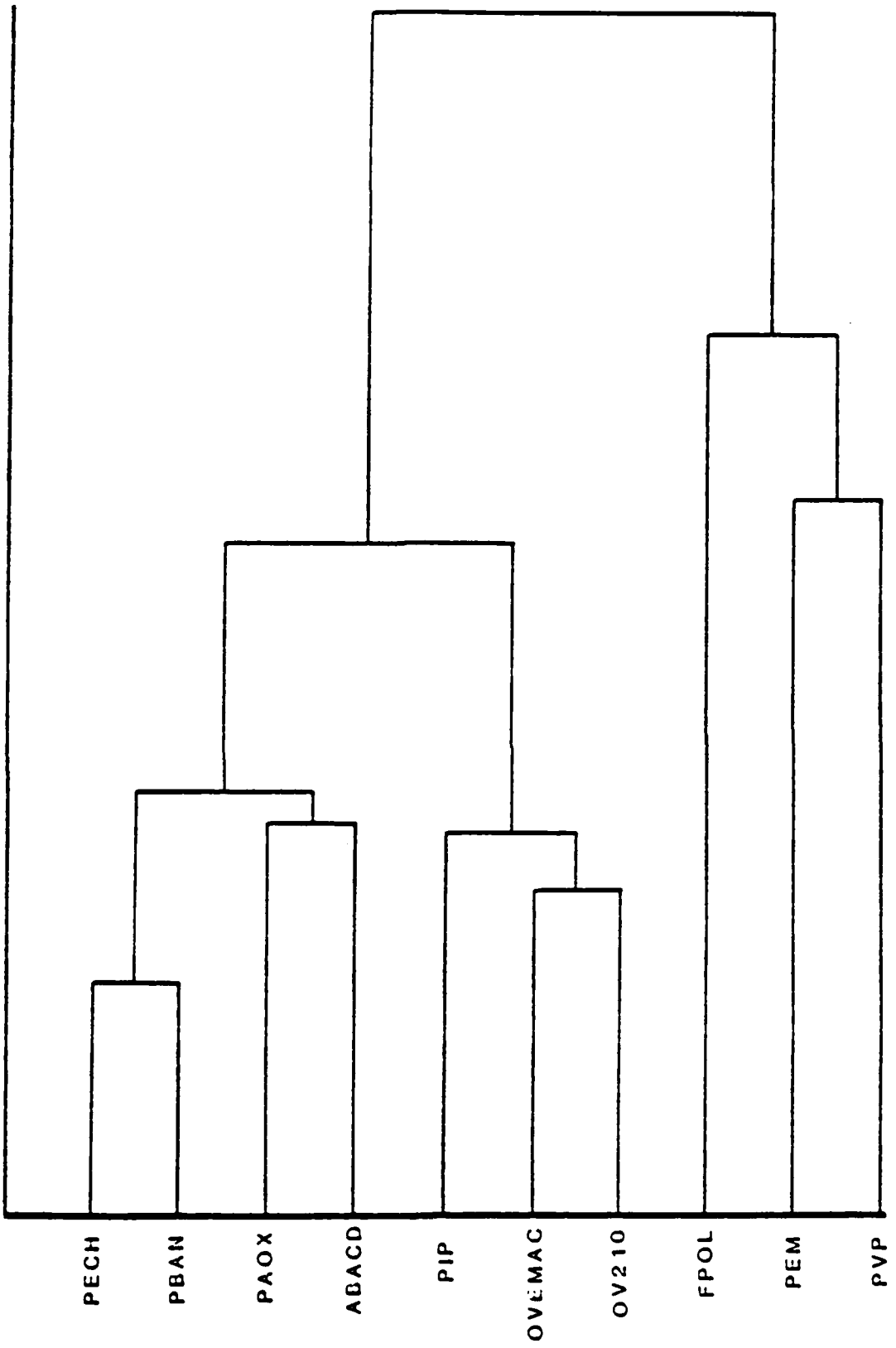

Fig. 7 — Typical hierarchical cluster results of coatings based on responses to 11 vapors (Euclidean distance metric with flexible fusion)

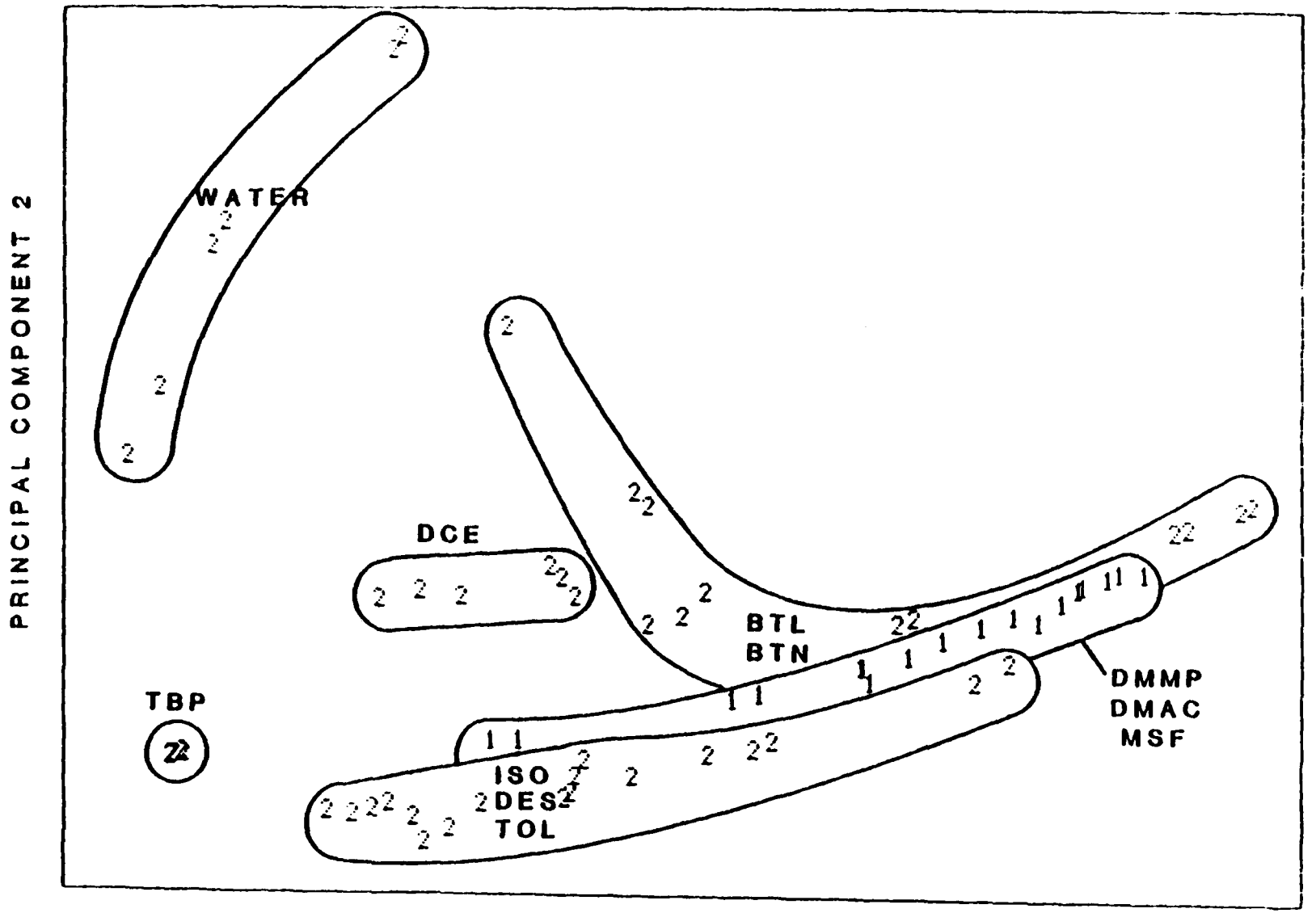

Fig. 8 — Principal component plot using results from 4 best coatings: PEM, FPOL, PVP, OVEMAC

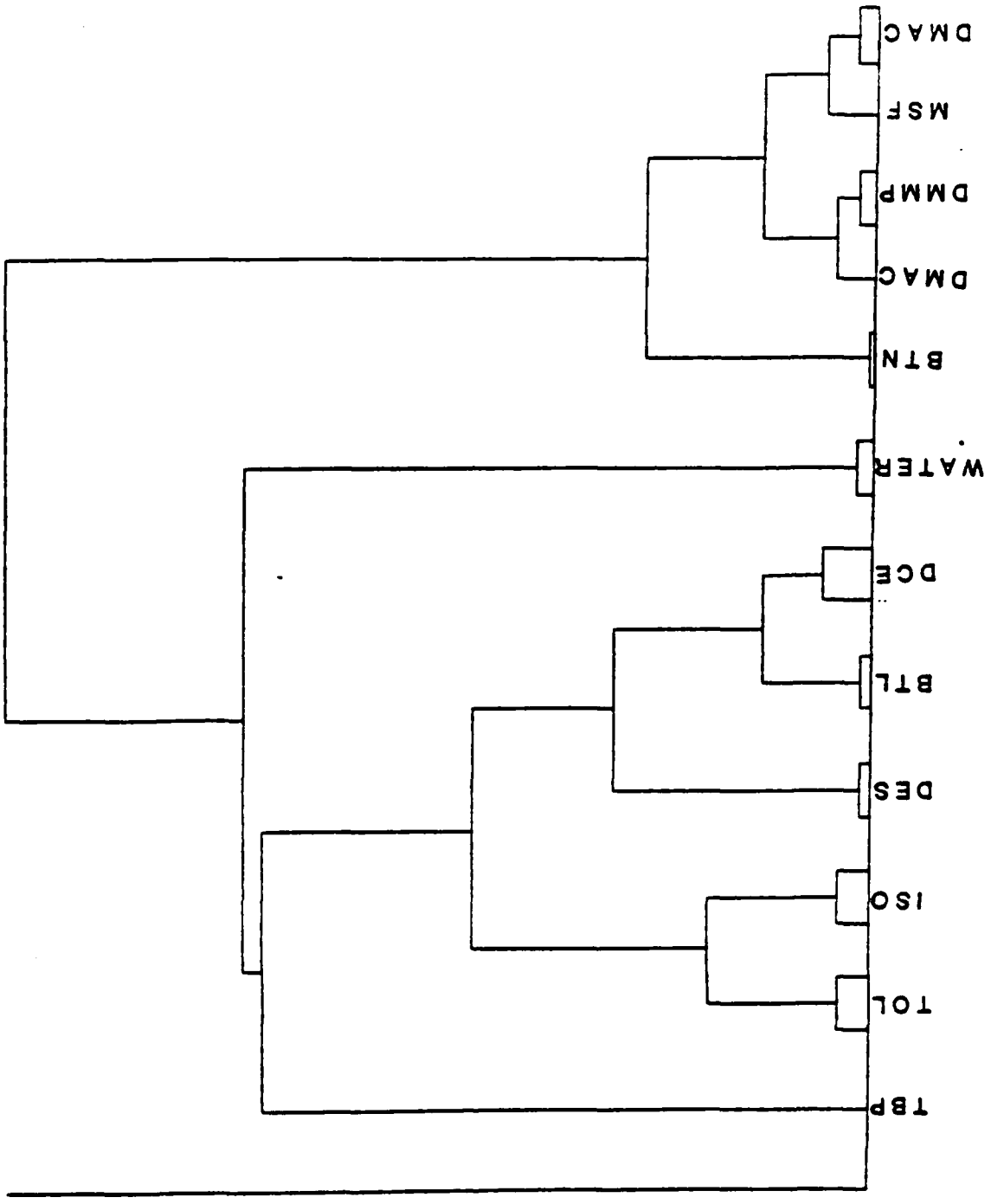

Fig. 9 — Typical hierarchical cluster results of the vapors for the best 4 coatings (Euclidean distance metric with flexible fusion

Appendix
ADDITIONAL SENSOR RESPONSE FIGURES

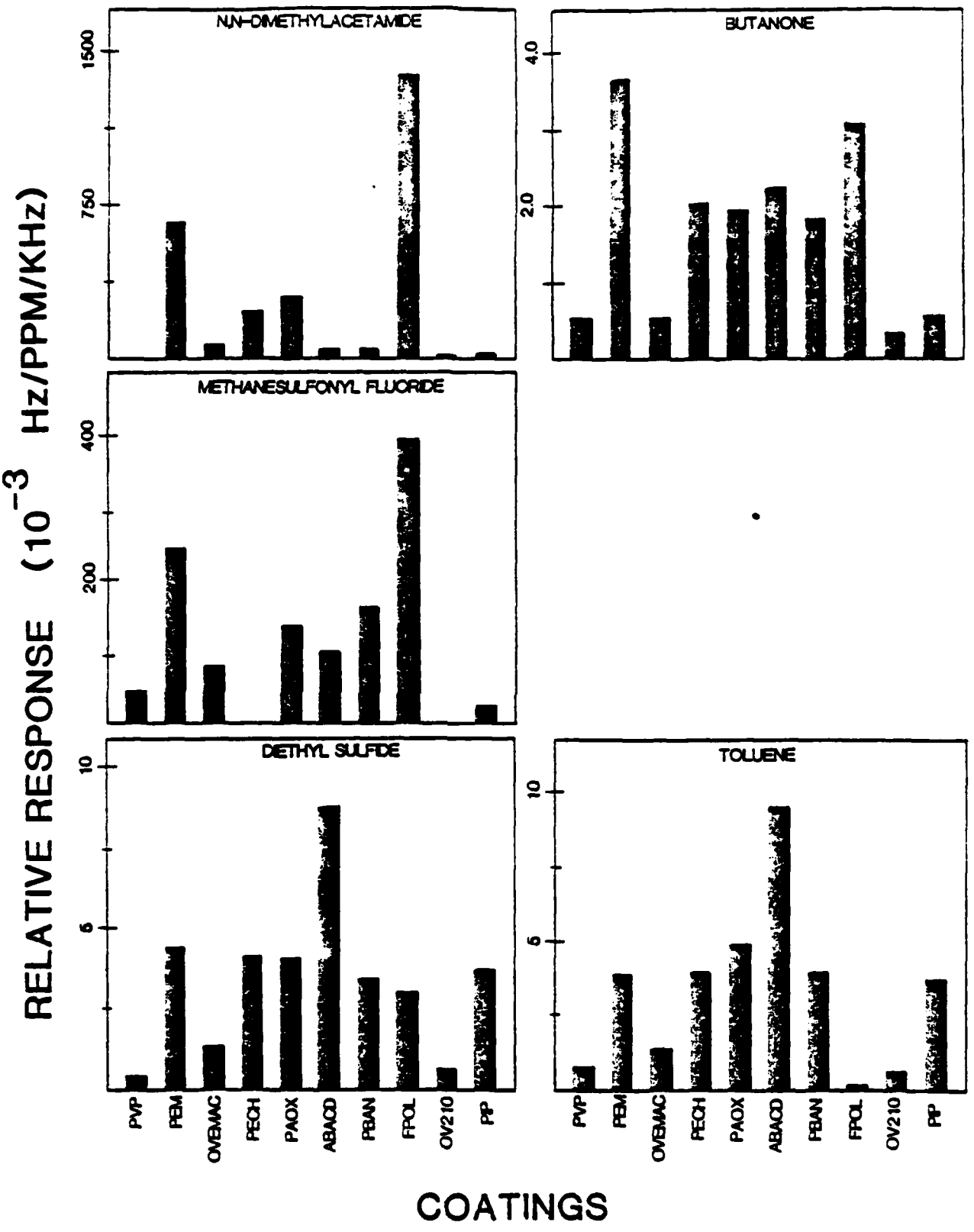
N,N-DIMETHYLACETAMIDE
1500
750
BUTANONE
4.0
2.0
METHANESULFONYL FLUORIDE
400
200
DIETHYL SULFIDE
10
6
TOLUENE
10
6
RELATIVE RESPONSE (10^-3 Hz/PPM/KHz)
PVP
PBM
OVBMAC
PECH
PAOX
ABACD
PBAN
FPOL
OV210
PIP
COATINGS

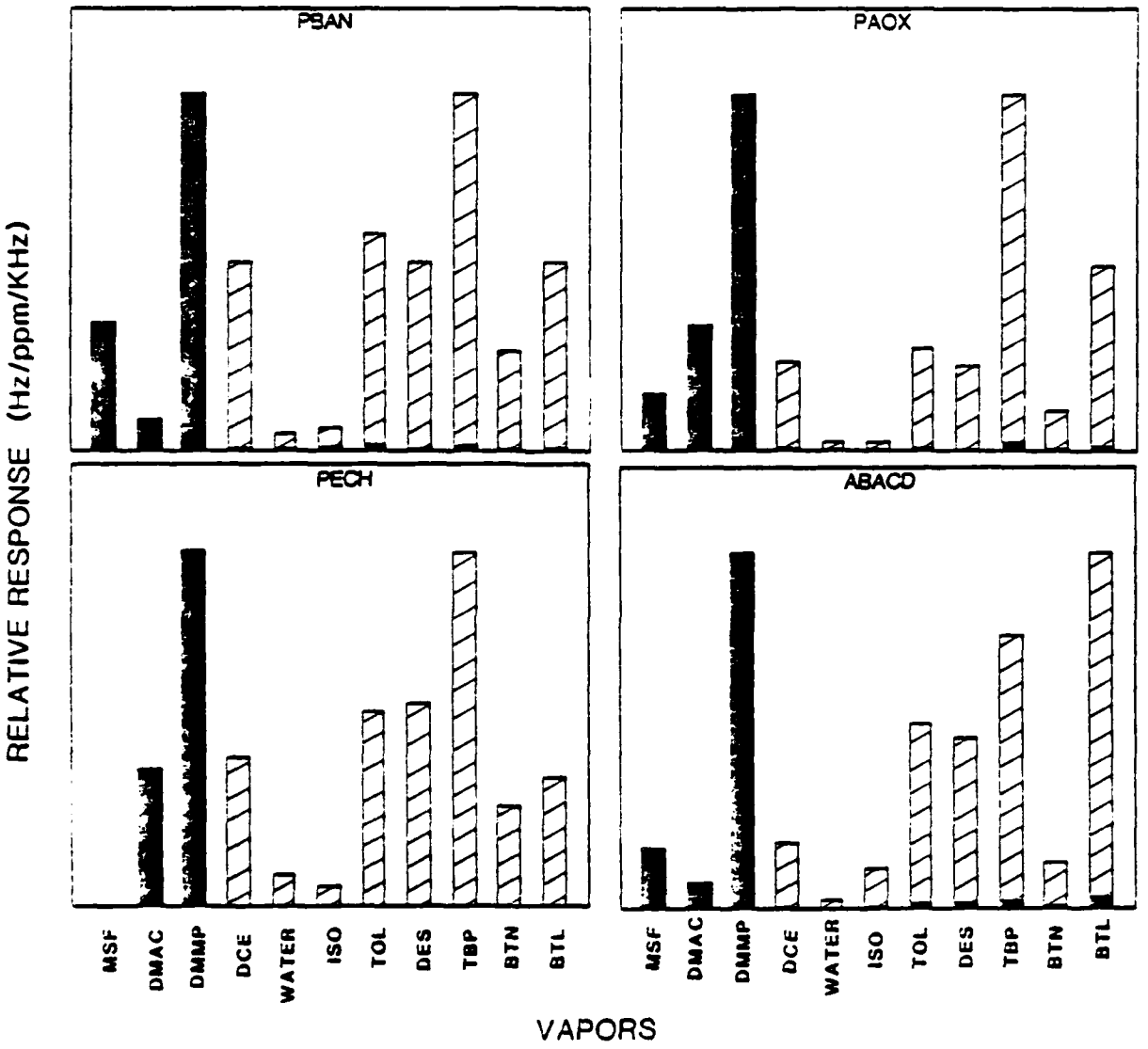
PBAN
PAOX
PECH
ABACD
RELATIVE RESPONSE (Hz/ppm/KHz)
MSF
DMAC
DMMP
DCE
WATER
ISO
TOL
DES
TBP
BTN
BTL
VAPORS

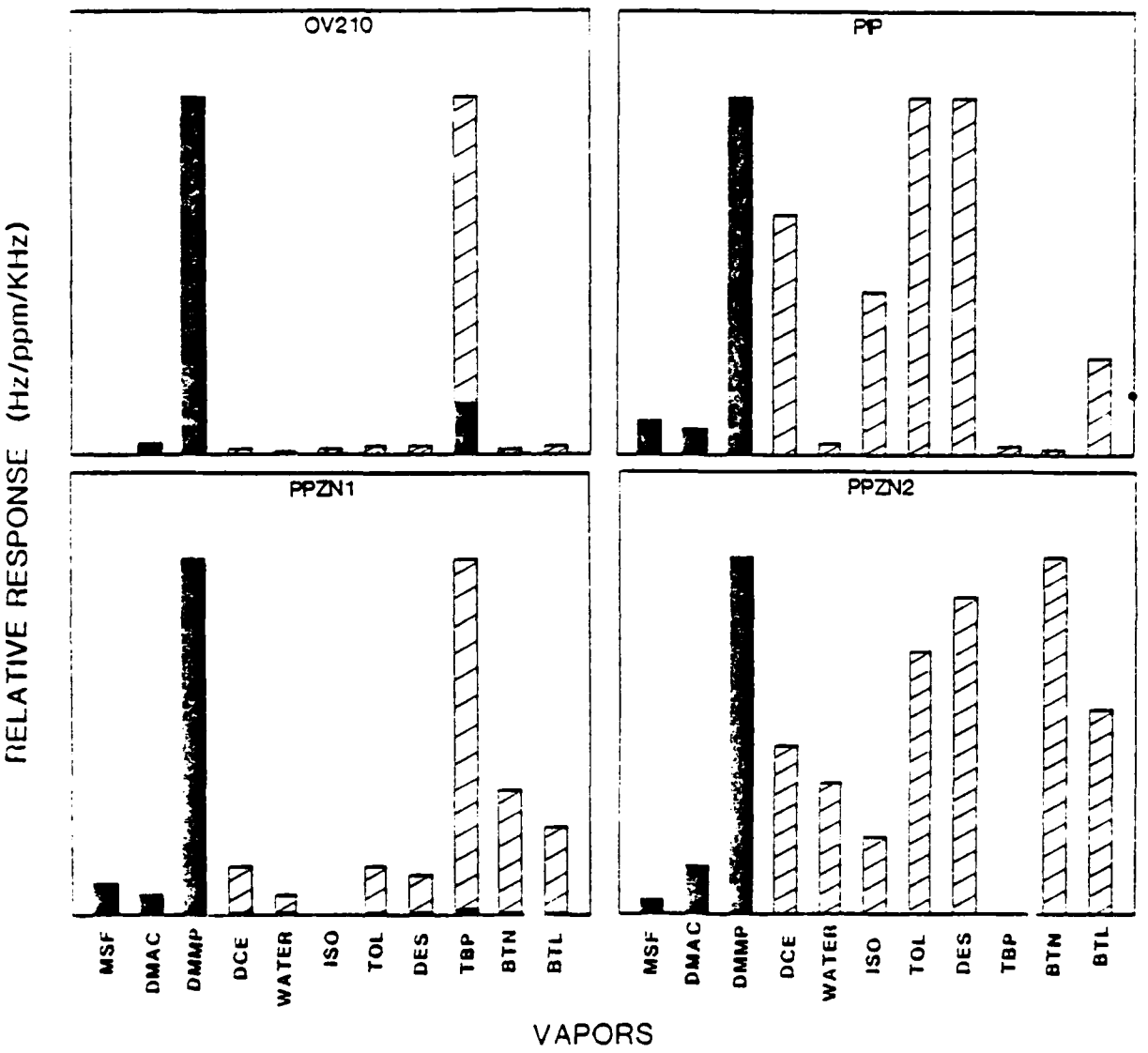
OV210
PIP
PPZN1
PPZN2
RELATIVE RESPONSE (Hz/ppm/KHz)
MSF
DMAC
DMMP
DCE
WATER
ISO
TOL
DES
TBP
BTN
BTL
VAPORS

END

10-86

DTIC